Aquatic Toxicology 99 (2010) 56–64

Contents lists available at ScienceDirect

Aquatic Toxicology

journal homepage: www.elsevier.com/locate/aquatox

Natural sunlight and residual fuel oils are an acutely lethal combination for fish embryos

Kristin Hatlen, Catherine A. Sloan, Douglas G. Burrows, Tracy K. Collier, Nathaniel L. Scholz, John P. Incardona*

Environmental Conservation Division, Northwest Fisheries Science Center, National Oceanic and Atmospheric Administration, 2725 Montlake Blvd E, Seattle, WA 98112, USA

ARTICLE INFO

Article history:
Received 1 February 2010
Received in revised form 29 March 2010
Accepted 1 April 2010

Keywords:
Oil spills
PAHs
Heterocyclic compounds
Phototoxicity

ABSTRACT

The majority of studies characterizing the mechanisms of oil toxicity in fish embryos and larvae have focused largely on unrefined crude oil. Few studies have addressed the toxicity of modern bunker fuels, which contain residual oils that are the highly processed and chemically distinct remains of the crude oil refinement process. Here we use zebrafish embryos to investigate potential toxicological differences between unrefined crude and residual fuel oils, and test the effects of sunlight as an additional stressor. Using mechanically dispersed oil preparations, the embryotoxicity of two bunker oils was compared to a standard crude oil from the Alaska North Slope. In the absence of sunlight, all three oils produced the stereotypical cardiac toxicity that has been linked to the fraction of tricyclic aromatic compounds in an oil mixture. However, the cardiotoxicity of bunker oils did not correlate strictly with the concentrations of tricyclic compounds. Moreover, when embryos were sequentially exposed to oil and natural sunlight, the bunker oils produced a rapid onset cell-lethal toxicity not observed with crude oil. To investigate the chemical basis of this differential toxicity, a GC/MS full scan analysis was used to identify a range of compounds that were enriched in the bunker oils. The much higher phototoxic potential of chemically distinct bunker oils observed here suggests that this mode of action should be considered in the assessment of bunker oil spill impacts, and indicates the need for a broader approach to understanding the aquatic toxicity of different oils.

Published by Elsevier B.V.

1. Introduction

The largest oil spills typically result from accidents involving the transport of large volumes of crude oil. Prominent examples include the 1989 *Exxon Valdez* oil spill in Alaska (37,000 tons of oil) and the 2007 *Hebei Spirit* oil spill in South Korea (10,800 tons). The *Exxon Valdez* spill in particular spurred two decades of ecotoxicology research on crude oil, with an emphasis on petrogenic polycyclic aromatic compounds (PACs). As a result, the *Exxon Valdez* spill is by several measures the most intensively studied oil spill in history, and there is now a large literature focusing on the toxicity of Alaska North Slope crude oil (ANSCO) carried by that ship (Peterson et al., 2003). Many of these studies focused primarily on the impacts to the early life history stages of fish and the underlying toxic mechanisms, identifying subsets of PACs with specific toxicodynamic properties linked to the most obvious responses in fish embryos to ANSCO exposure (Carls and Meador, 2009). Much less is known, however, about the toxic mechanisms that may be associated with oils that are chemically distinct from ANSCO. This includes, for example, the toxicity of residual fuel oils that are burned to power large vessels ("bunker" oils). Given the relatively high frequency of vessel accidents and losses around the world, bunker oil toxicity warrants greater study, despite the smaller scale of most bunker oil spills.

Studies on ANSCO have led to a model in which component PACs are the primary consideration for an oil's toxicity. However, a handful of studies on residual fuel oils have provided evidence of toxic activities unattributable to constituent PACs alone (Barron et al., 1999; González-Doncel et al., 2008; Neff et al., 2000). Due to the nature of modern refinery practices, residual fuel oils have chemical compositions that are distinct from those of unrefined crude oils, and even from those of bunker oils of previous decades (Uhler et al., 2007). Residual fuel oils are by definition the end-products of the refining process, and often have been subjected to conversion processes such as catalytic cracking (Matar and Hatch, 2001). Bunker fuels, the generic term applied to fuel stored onboard ships, typically consist of a highly viscous heavy residual fuel oil that is mixed with a lighter fuel (typically diesel), to facilitate pumping and flow. For example, one of the most common bunker fuel classes is intermediate fuel oil (IFO) 380, which is a residual oil cut

Abbreviations: ANSCO, Alaska North Slope crude oil; IFO, intermediate fuel oil; MDO, mechanically dispersed oil; PACs, polycyclic aromatic compounds.

* Corresponding author. Tel.: +1 206 860 3347; fax: +1 206 860 3335.
E-mail address: john.incardona@noaa.gov (J.P. Incardona).

0166-445X/$ – see front matter. Published by Elsevier B.V.
doi:10.1016/j.aquatox.2010.04.002

EX5038-000001-TRB

with roughly 3% marine gasoil (equivalent to no. 2 diesel) to produce a viscosity of 380 centistokes. Many chemical and elemental components of crude oil are much more highly concentrated in residual oils (Clark and Brown, 1977; Uhler et al., 2007; Wang et al., 2003). Residual fuel oils and mixed products such as IFO 380 have a higher percentage of aromatic compounds, a higher total mass of PACs and, importantly, fractions of uncharacterized polar compounds (an "unresolved complex mixture") that can approach 30% of the mass (Clark and Brown, 1977). Residual fuel oils also are often enriched with a higher content of metals such as nickel and vanadium (Matar and Hatch, 2001). Moreover, there is an overall high degree of chemical heterogeneity among modern residual fuel oils from different sources (Uhler et al., 2007).

We previously explored mechanisms underlying the toxic effects of ANSCO and individual PACs in a series of studies using zebrafish embryos (Carls et al., 2008; Incardona et al., 2004, 2005, 2006). These studies showed that various waterborne preparations of ANSCO containing only dissolved constituents, or dissolved constituents together with whole oil droplets or particulate oil, produced a characteristic and highly reproducible syndrome of developmental abnormalities in fish embryos. This "canonical" crude oil toxicity is marked primarily by pericardial and yolk sac edema, which results from cardiac dysfunction due to directly cardiotoxic constituents consistent with the activities of the most abundant PACs in ANSCO, specifically, the tricyclic fluorenes, dibenzothiophenes, and phenanthrenes (Carls et al., 2008; Incardona et al., 2004, 2005, 2009). Other toxic effects in zebrafish embryos resulting from ANSCO exposure included intracranial hemorrhage and blister-like malformations of the finfolds (Incardona et al., 2005), but the precise etiology of these effects is unknown. These findings reflect the inherent toxicity of ANSCO in the absence of other stressors.

There is also large literature demonstrating that certain PACs are capable of producing cellular phototoxicity through the UV-mediated activation of bioaccumulated compounds and subsequent generation of reactive oxygen species and membrane damage (Arfsten et al., 1996; Yu, 2002). This has been raised as a mechanism that is putatively important in the environment, due to the potential susceptibility of unpigmented organisms to UV exposure from solar radiation in shallow waters (Barron and Ka'aihue, 2001). Most of the studies on PAC phototoxicity in aquatic systems have focused on planktonic invertebrates e.g. (Cleveland et al., 2000; Duesterloh et al., 2002; Pelletier et al., 1997), while only a few have focused on phototoxicity of individual PACs and ANSCO preparations in fish early life history stages (Barron et al., 2003; Diamond et al., 2006; Farwell et al., 2006; Oris and Giesy, 1987). To date there is no systematic comparative toxicity study in fish early life history stages that has included modern marine residual fuel oils with and without additional stressors such as natural sunlight.

Here we begin to elucidate potential toxic differences among oil types by directly comparing the effects of exposing zebrafish embryos to similar preparations of ANSCO and two IFO 380s originating from different ports, with and without the influence of natural sunlight. The PAC fractions of the whole oils were analyzed and compared to the waterborne PAC composition of mechanically dispersed oil (MDO) preparations (Carls et al., 2008) used in exposures. In addition, a number of waterborne compounds were identified that were markedly enriched in the IFO 380s relative to ANSCO.

2. Materials and methods

2.1. Mechanically dispersed oil (MDO) preparations

The ANSCO was obtained from the NOAA Auke Bay Laboratory as previously described (Carls et al., 2008; Incardona et al., 2005, 2009). The crude oil was subjected to partial artificial weathering by heating at 65 °C until reduced volumetrically by 20% (by mass). One of the IFO 380s, IFO1, was obtained from the California Department of Fish and Game's Office of Spill Prevention and Response. The other IFO 380, IFO2, was obtained from Olympic Tug and Barge in the Port of Seattle. Originating from different suppliers, these two IFO 380s were likely derived from different crude oil stocks, with IFO2 probably derived from an Alaska North Slope product. MDOs are in essence small-scale (e.g. 100-ml) preparations comparable to a high energy water accommodated fraction (WAF), in which oil and water are agitated to disperse the oil, followed by a one-hour separation period allowing coalescence of droplets on the surface. The resulting water beneath the surface carries a mixture of dissolved oil components as well as some remaining uncoalesced droplets or microdroplets of whole oil. MDOs prepared by manual shaking in separatory funnels (Carls et al., 2008) have been shown to produce comparable water chemistry to large-scale (e.g. 40-l) high energy WAFs (Barron et al., 2003; Incardona et al., 2005). For these studies, a small mass of oil was added to 100 ml of zebrafish system water (Linbo, 2009) in a separatory funnel and shaken to disperse the oil into fine droplets or particles. Due to the difficulty of volumetrically delivering microliter quantities of viscous oil, micropipets were calibrated to reproducibly deliver a drop of desired mass, either 2 mg or 5 mg. Several MDOs were prepared for embryo exposures by delivering a 2- or 5-mg drop of oil to the surface of 100 ml zebrafish system water in a 1-l glass separatory funnel. For PAC analytical chemistry, MDOs were prepared by weighing 12.5 mg oil onto a glass coverslip. The coverslip was then placed into the separatory funnel with 100 ml zebrafish system water. All MDOs were systematically prepared by shaking vigorously for 5 min, followed by 1 h of separation. Whereas visual inspection of the ANSCO and IFO2 MDOs revealed complete oil dispersion, the IFO1 drop adhered to the vessel side with a remaining fraction still visible at the end of shaking. All MDOs had entrained droplets/particles of oil as indicated by microscopic inspection (data not shown). The reproducibility of MDO preparation for the two IFO 380s was determined biologically (see below) and chemically (Supplementary Fig. S1).

2.2. Analytical chemistry

PACs were analyzed for all MDOs from two experiments; additional compounds were identified in the MDOs from one of these. Aliquots from each MDO were removed for embryo exposures and then the remaining MDO portions were each filtered through no. 1 Whatman paper to partially remove particulate oil. Each filtrate was then stored in brown glass bottles containing 20 ml dichloromethane until analysis. For quality assurance, a blank water sample and a spiked blank water sample were prepared in brown glass bottles, both containing 250 ml of zebrafish system water and 20 ml of dichloromethane, with a known mixture of PACs (3000 ng each analyte) added to the spiked blank. After addition of surrogate standards (1080 ng each of D8-naphthalene, D10-acenaphthene and D12-benzo[*a*]pyrene in 600 μl of isooctane), each sample was transferred to 1-l separatory funnel. Samples were extracted by shaking with dichloromethane for 2 min followed by 2-min separation time. After collecting the dichloromethane phase, the samples were extracted a second time with another 20 ml of dichloromethane and the two extracts were combined. Sodium sulfate (5 g) was added to each sample, the samples were allowed to sit overnight, then more sodium sulfate (5 g) was added.

To quantify selected PACs, a 3-ml aliquot of each extract was exchanged from dichloromethane to isooctane while being concentrated to 100 μl, then analyzed using gas chromatography/mass spectrometry (GC/MS) selected ion monitoring as described previously (Sloan et al., 2005) with additional monitoring for alkylated

PACs. Analyte concentrations in the water (μg/l) were calculated using surrogate standards and six concentration levels of GC/MS calibration standards ranging from 0.004 to 1.0 ng/μl for each analyte. For each analyte, the concentration evoking the peak response in the lowest level calibration standard was used to calculate the lower limit of quantitation (LOQ). LOQs ranged from approximately 0.02 to 0.2 μg/l. Surrogate standard recoveries ranged from 83 to 94%, and the spiked blank recoveries ranged from 106 to 124%. The method blank contained 0.72 μg/l total low molecular weight PACs (naphthalenes, fluorenes and phenanthrenes), whereas the high molecular weight PACs in this sample were all below the LOQs.

For the identification of additional oil-related compounds, 1 ml aliquot of each extract was exchanged from dichloromethane to isooctane while being concentrated to 100 μl, then analyzed using GC/MS scanning at 50–600 Da. The GC/MS system included an Agilent 5973 Mass Selective Detector, an Agilent 5890 GC with on-column injection and a J&W 60 m × 250 μm DB-5 column (0.25-μm film-thickness). Software used for data acquisition and compound identification included Agilent Chemstation, National Institute of Standards and Technology (NIST) library and the Automated Mass Spectral Deconvolution and Identification System (AMDIS). For each visible peak on the chromatogram, the spectrum from the nearest baseline was subtracted from the top of the peak. The resultant background-subtracted spectrum was compared to the NIST library for the most appropriate match. When a member of an alkyl aromatic family of compounds was identified (e.g. C1 carbazole), the chromatogram was examined for additional homologs belonging to that family (e.g. C2 carbazole, C3 carbazole, etc.). Because the full range of n-alkanes could be found in all samples, Kovats indices (Kováts, 1958, 1965) were calculated for all identified peaks. (The calculation of the Kovats retention index, I_x, of a compound X is:

$$I_x = 100 \times \frac{T_n - T_x}{T_{n+1} - T_n} + 100n$$

where T_x is the retention time of compound X. T_n and T_{n+1} are the retention times of the n-alkanes with carbon numbers n and $n+1$ which bracket the compound X.)

The chromatograms of the extracts were searched for additional compounds with known Kovats indices that might be found in the water-soluble fraction of oil. Once a compound was detected in an extract chromatogram, the chromatograms of the other extracts were screened for the same compound. Without standards, it was not possible to precisely determine the concentrations of these compounds. Instead, a "quantitation" ion was chosen for each analyte (usually the molecular ion or the largest ion) and the integrated peak area for that ion was measured. This peak area was divided by the peak area of the surrogate standard D10-acenaphthene in that extract to produce a normalized ion area. Compounds that were present in both the sample blank and oiled water extracts at approximately the same level (or lower) for the latter were excluded from further analysis.

Whole oil samples were prepared for quantifying selected PACs by diluting 100 mg of oil plus surrogate standards (2700 ng each of D8-naphthalene, D10-acenaphthene and D12-benzo[*a*]pyrene in 1.5 ml of isooctane) to 10 ml in dichloromethane. A 200 μl aliquot of each oil sample was further diluted to 3.35 ml in dichloromethane and then cleaned up by gravity-flow silica/alumina chromatography columns and size-exclusion high performance liquid chromatography as previously described (Sloan et al., 2005). The samples were analyzed by GC/MS as described above for the oiled water extracts. Analyte concentrations in the oil (ng/mg) were calculated using the surrogate standards and eight concentration levels of GC/MS calibration standards ranging from 0.004 to 10 ng each analyte/μl. Surrogate standard recoveries, taking into account the portion of sample analyzed, ranged from 85 to 124%.

2.3. Zebrafish embryo exposure

MDO preparations were made for eight independent exposure experiments conducted between late July and mid-December; five of these included phototoxicity assays. Adult zebrafish were maintained and embryos collected as described elsewhere (Linbo, 2009). To assess a potential protective role of pigment in sunlight exposures, some experiments utilized *nacre* embryos, which have a marked reduction in melanophores (Lister et al., 1999). Duplicate or triplicate groups of 20 embryos were exposed beginning 4–6 h post-fertilization (hpf) in pre-cleaned 30-mm glass Petri dishes. Aliquots of MDOs (15 ml) were added to the Petri dishes, and embryos were then transferred into treatment solutions in a small volume (~100 μl) of zebrafish system water. Exposures were carried out in a laboratory incubator without light at 28.5 °C, and embryos incubated up to 72 hpf without renewal of exposure water. Controls were incubated in clean zebrafish system water in the same incubator. Pericardial edema was scored at 48 hpf or 72 hpf. Subsamples of developing embryos were removed at 24, 48, and 72 hpf for exposure to natural sunlight. There were two types of negative control for sunlight exposure: one exposed to clean water and sunlight, and one exposed to oil and ambient outdoor temperature shaded from sunlight. Typically, 10–15 embryos were removed from each replicate exposure dish and placed in a new Petri dish with clean system water and then transported outdoors in a shallow plastic tray on a handcart. Petri dishes were left uncovered for the duration of sunlight exposure, and gently agitated occasionally to evenly disperse the embryos. Negative controls for sunlight exposure experienced the same outdoor ambient temperature, covered loosely with aluminum foil and shaded on the lower shelf of the cart; water temperature was not recorded. In order to compare experiments performed under different weather conditions, nominal UV exposure was estimated using a Macam UV203 radiometer (Advanced Photonics International, Inc., Fairfield, CT). The radiometer was used in average mode to obtain average UV-A and UV-B levels for the entire sunlight exposure duration. UV-A levels were measured for the first half of the exposure, and UV-B levels during the second half. Sunlight exposure ranged from 20 min on partly cloudy summer days to 2 h on overcast winter days (Table 1). Two of the phototoxicity experiments utilized the *nacre* mutant with

Table 1
Summary of sunlight exposure conditions.

Date (experiment no.)	Weather	UV-A (mW/m^2)	UV-B (mW/m^2)	Duration (min)	UV-A/UV-B dose (μW h/cm^2)	Nominal oil dose (ppm)[a]
31 July (experiment 1)	Sunny	18,670	1805	10	311/30	20
1 October (experiment 2)	Cloudy	8590	294	20	286/10	20
7 October (experiment 3)	Rainy	4611	469	120	922/94	50
22 October (experiment 4)	Sunny	8971	420	120	1794/84	50
4 December (experiment 7)	Cloudy	3421	ND	120	684/ND	125

ND = not determined.
[a] By mass of whole oil dispersed in water.

Table 2
PAC concentrations and composition of MDO preparations.[a].

Oil	Assay		∑PACs	∑NPHs	∑FLUs	∑DBTs	∑PHNs	∑FLAs	∑CHRs	∑5–6
ANSCO	Edema + phototoxicity	Concentration (μg/l)	210	154.0	11.7	16.9	24.1	0.6	3.0	0.09
		Composition (% of ∑ PACs)		73.3	5.6	8.0	11.5	0.3	1.4	0.04
	Edema	Concentration (μg/l)	340	249.0	19.1	27.9	40.1	1.1	5.3	0.2
		Composition (% of ∑ PACs)		73.2	5.6	8.2	11.8	0.3	1.6	0.06
IFO1	Edema + phototoxicity	Concentration (μg/l)	240	160.0	10.7	11.4	40.8	3.4	8.6	0.5
		Composition (% of ∑ PACs)		66.7	4.5	4.8	17.0	1.4	3.6	0.2
	Edema	Concentration (μg/l)	100	65.2	4.8	4.7	17.1	1.3	3.7	0.2
		Composition (% of ∑ PACs)		65.2	4.8	4.7	17.1	1.3	3.7	0.2
IFO2	Edema + phototoxicity	Concentration (μg/l)	440	318.0	17.1	20.3	53.9	4.2	13.4	0.9
		Composition (% of ∑ PACs)		72.3	3.9	4.6	12.3	0.9	3.0	0.2
	Edema	Concentration (μg/l)	310	229.0	13.2	14.4	38.5	2.7	8.6	0.5
		Composition (% of ∑ PACs)		73.9	4.3	4.6	12.4	0.9	2.8	0.2

[a] Data are for MDOs from experiments 7 and 8. ∑PACs is the sum of all 39 analytes (shown in Figure S1), ∑NPHs, etc. are the sums of the parent compound and each alkylated homologue, and ∑5–6 is the sum of seven 5-ring and one 6-ring analytes. NPHs, naphthalenes; FLUs, fluorenes; DBTs, dibenzothiophenes; PHNs, phenanthrenes; FLAs, fluoranthenes; CHRs, chrysenes.

reduced pigment. At the end of sunlight exposure, embryos were immediately returned to the lab and examined microscopically. Embryos were imaged with a Nikon SMZ800 stereomicroscope and Fire-i 400 video camera (Unibrain, Inc., San Ramon, CA). Edema was scored as mild, moderate, or severe, but is reported here as either present or absent. Tail defects in sunlight-exposed embryos were scored as rounding of cells in the outer finfold, rounding of cells in the inner finfold, lysis of cells in the outer finfold, and lysis of cells in the inner finfold or tail tissue.

3. Results

3.1. Chemical composition of MDO preparations

Aqueous concentrations of selected PACs were analytically determined for MDO preparations used for two experiments (Table 2 and Supplementary Fig. S1), and assayed for edema and phototoxicity, and edema only, respectively. The MDO filtrates would have contained some oil microdroplets (Carls et al., 2008; Payne et al., 1999), and based on these previous studies, we estimate that dissolved phase compounds represented roughly 20% of the total measured PACs. Consistent with this, each MDO analysis showed a relative enrichment with compounds that were more water-soluble relative to the source oils (Fig. S1). These included the naphthalenes as well as the parent and lower alkylated fluorenes, dibenzothiophenes and phenanthrenes. For example, the ratios of phenanthrene to C4-phenanthrene in the source oils were 1.0, 0.45, and 0.52 for ANSCO, IFO1, and IFO2, respectively, while the mean ratios in the respective MDO preparations were 2.3, 1.1, and 1.8. There was also a relative reduction in the higher molecular weight chrysenes. The PAC composition was highly reproducible between different MDO preparations using the same oil (Table 2, Fig. S1). Although the concentrations of PAC subclasses and summed PAC (∑ PACs) were more variable between preparations constituted on different days, all of the preparations fell within a range of 100–440 μg/L ∑ PACs (Table 2).

As an initial step towards identifying differences between the unrefined ANSCO and the residual IFOs, a GC/MS full scan analysis was carried out on extracts of MDO preparations from one phototoxicity experiment (#7, Table 1). Identified compounds are listed individually in Supplementary Table S1. These consisted of 45 alkanes, 378 aromatic hydrocarbons with their alkylated families, 35 nitrogen heterocycles with their alkylated families (primarily carbazoles), 32 various oxygen containing compounds, 81 sulfur heterocycles and their alkylated families, and 4 large unidentified peaks. Because of the lack of available quantification standards for these compounds, we were unable to calculate actual concentrations. Rather, it was only possible to compare the normalized ion

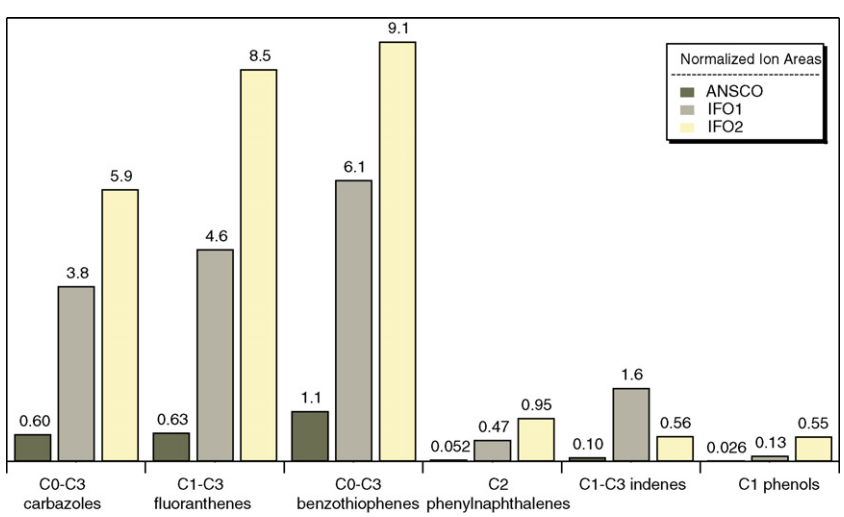

Fig. 1. Normalized ion areas for compound classes enriched in IFO 380 MDO preparations relative to ANSCO identified in full scan GC-MS analysis. Ion areas were summed for families of compounds that had chromatographic peaks at least 5 times larger in the IFO 380 MDO extracts compared to the ANSCO MDO extract. Ion area ratios for individual subfamilies are listed in Table S2.

Table 3
Summary of compounds of interest in the full scan analysis of oiled water extracts.

Chemical group	Compound	Number of isomers	IFO1 to ANSCO peak area ratio[a]	IFO2 to ANSCO peak area ratio[a]
Aromatic hydrocarbons				
Benzenes	1,1′-Butylidene-bis-benzene (tentative)	1	19.015	39.216
	C3 benzene	5	3.945	2.555
Indans	Indan	1	4.582	4.672
	C1 indan	4	2.201	3.262
Indenes	Indene	1	43.402	0.000
	C1 indene	2	48.868	8.961
	C2 indene/C1 dihydronaphthalene	7	9.405	4.054
	C3 indene	3	6.371	6.008
Naphthalenes	C3 alkenyl naphthalene	5	5.121	8.183
Dihydronaphthalenes	1,2-Dihydronaphthalene	1	14.613	0.000
Phenyl naphthalenes	C1 phenyl naphthalene/C3 alkenyl phenanthrene/anthracene	6	2.754	3.400
	C2 phenyl naphthalene/C4 alkenyl phenanthrene/anthracene	6	9.092	18.334
Acenaphthene	Acenaphthene	1	5.080	0.943
Phenanthrenes/Anthracenes	C4-phenanthrene/anthracene	15	3.259	3.528
Dihydrophenanthrenes/ Dihydroanthracenes	Dihydrophenanthrene/ dihydroanthracene	2	2.338	4.361
Fluoranthenes/Pyrenes/ Benzofluorenes	Fluoranthene/pyrene	2	8.325	7.206
	Benzo[*b*]fluorene	1	6.853	6.937
	C1 fluoran-thene/pyrene/benzofluorene	6	6.325	7.844
	C2 fluoran-thene/pyrene/benzofluorene	14	6.505	16.912
	C3 fluoran-thene/pyrene/benzofluorene	11	12.207	16.420
Benz[a]anthracenes/Chyrsenes	C1 benz[*a*]anthracene/chyrsene	7	3.313	5.635
	C2 benz[*a*]anthracene/chyrsene	10	3.615	6.003
Nitrogen heterocyclics				
Indoles	C2 indole (tentative)	1	1.881	3.771
Carbazoles	Carbazole	1	6.526	10.163
	C1 carbazole	4	7.651	13.049
	C2 carbazole	11	6.808	11.132
	C3 carbazole	12	5.334	7.582
	C4 carbazole	6	3.833	3.148
Oxygen containing hydrocarbons				
Benzaldehydes	C4 benzaldehyde (tentative)	1	0.356	1.144
	Pentamethylbenzaldehyde	1	1.034	1.037
Phenols	C1 phenol	3	5.019	21.223
	C2 phenol	5	3.389	0.000
	C3 phenol	3	3.949	0.000
	C11 phenol	2	107.945	4.135
Alcohols	Phenylethyl alcohol	1	28.486	0.000
	Phenoxypropanol	1	28.681	0.000
Ethers	Diphenyldiethyl ether	2	58.171	0.000
Ketones	Benzoylacetone (tentative)	1	5.550	0.000
Sulfur heterocyclics				
Benzothiophenes	Benzothiophene	1	43.008	40.804
	C1 benzothiophene	4	22.426	29.463
	C2 benzothiophene	5	5.499	7.111
	C3 benzothiophene or C7 benzene	15	2.517	5.528
Benzonaphthothiophenes	Benzonaphthothiophene	3	1.353	4.042
Unidentified compounds				
	Unknown (191 ion)	1	3.608	0.000
	Unknown (247 ion; MW 318; maybe C16 phenol)	1	41.654	1.001
	Unknown (247 ion; possibly MW 318)	1	90.799	2.793
	Unknown (303 ion; MW 374)	1	77.027	1.866

[a] Ratio of normalized peak areas in extract compared to ANSCO normalized peak areas.

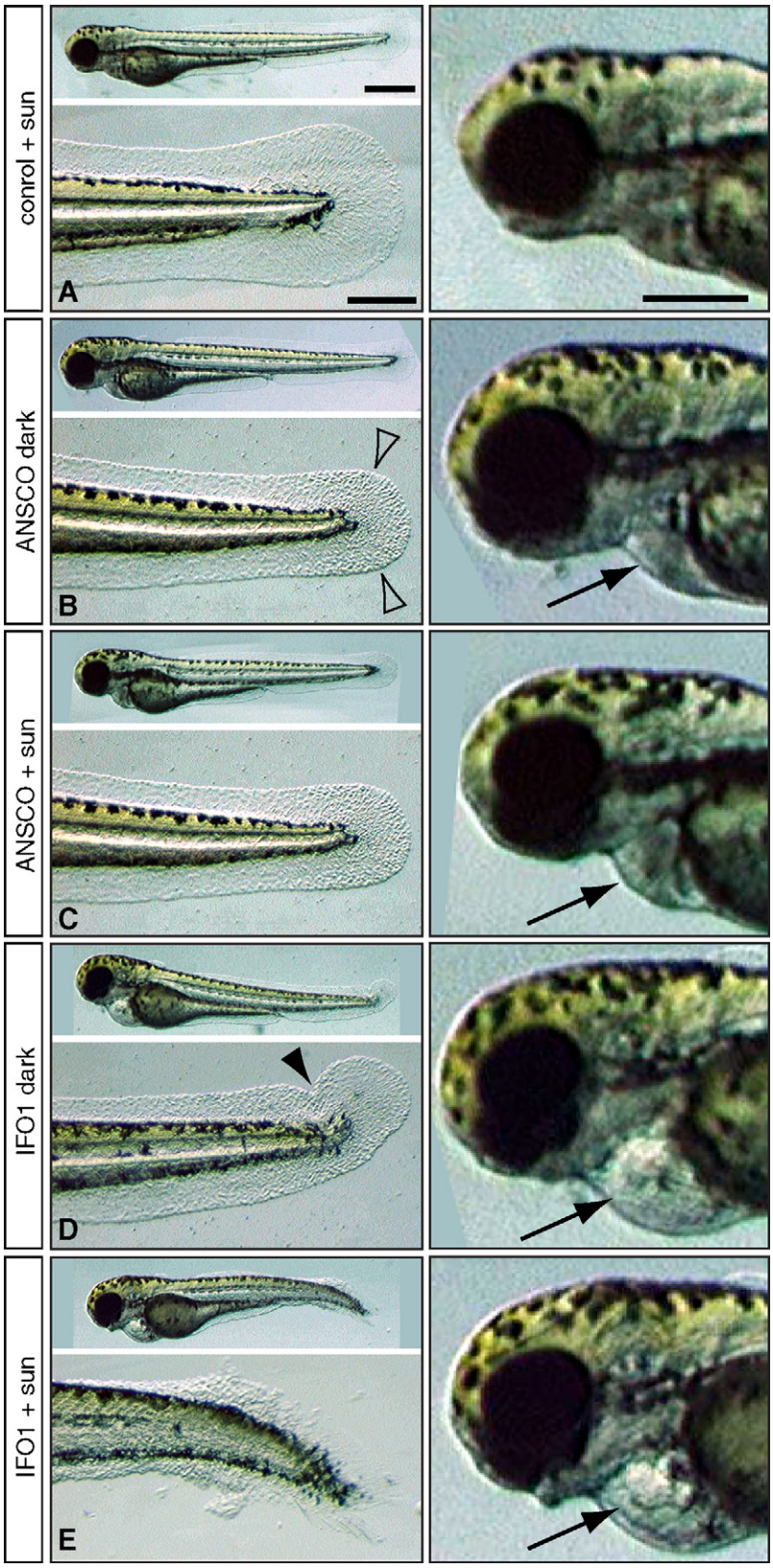

Fig. 2. Morphological effects of exposure to different oils. Embryos were exposed to the indicated MDO preparation from 6 to 72 hpf in the dark, exposed to sunlight or outdoor ambient temperature in the dark for 10 min, then returned indoors and imaged (experiment 1, 31 July). The top image in each panel shows the entire larva with the head to the left, while the lower left and right images show higher magnification views of the tail and pericardial region, respectively. Arrows indicate pericardial edema in oil-exposed embryos (B–E). Scale bars are 0.5 mm (top images) and 100 μm (lower and right images). (A) Larva exposed to clean water and sunlight. (B) Larva exposed to ANSCO without sunlight. Caudal finfold shows reduced growth (unfilled arrowheads). (C) Larva exposed to ANSCO followed by sunlight; note absence of tail necrosis. (D). Larva exposed to IFO1 without sunlight. Caudal finfold shows reduced growth and notch on dorsal side (arrowhead). (E) Larva exposed to IFO1 followed by sunlight; note striking loss of tail tissue to cytolysis. Images are representative of results from all experiments.

areas of a particular compound between the different extracts. The relative ion areas of the two IFO 380s compared to ANSCO are summarized for each family of compounds in Table 3. Notably, the analytical method used was likely unsuitable for the detection of polar compounds.

We focused primarily on the chromatographic peaks that were substantially larger (5 times or more) in the IFO1 and/or IFO2 extracts compared to the ANSCO extract. These compounds are summarized in Table S2. Some of the most prominent differences between the crude oil and IFOs included the following compounds, with normalized ion area sums displayed in Fig. 1: carbazole and C_1 to C_3 carbazoles (C0–C3 CBZs), C_1 to C_3 fluoranthenes/pyrenes (C1–C3 FLAs), benzo[*b*]thiophene and C_1 to C_3 benzothiophenes (C0–C3 BTPs), C_2 phenyl naphthalenes (C2 PhNPHs), C_1 to C_3 indenes (C1–C3 IDEs) and C_1 phenols (C1 PhOHs).

3.2. Comparable and novel sublethal toxicities of IFOs relative to ANSCO in the absence of sunlight

Overall, all three oils produced cardiovascular toxicity after incubation in the dark (Table 4). For all oil exposures in the absence of sunlight, embryos developed a high prevalence of pericardial edema by 48 hpf (data not shown, Table 4 and Fig. 2). Edema was qualitatively assessed in all experiments, and quantified in 4 experiments, where the frequency ranged from 81 to 90% (mean 88%) after exposure to ANSCO and 37–100% (mean 68%) for IFO1, and was 100% for IFO2 in all experiments. In the experiments for which PACs were analyzed (Table 2), edema was present in a lower percentage of embryos exposed to ANSCO relative to IFO1 despite a comparable or higher total PAC concentration. Although the edema response was qualitatively similar between ANSCO and IFO1, the corresponding concentrations of tricyclic PACs differed by a factor of three (87 μg/l vs. 27 μg/l respectively). Similarly, the IFO2 MDO from experiment 8 had total tricyclic PACs (66 μg/l) slightly lower than the ANSCO MDO (87 μg/l), but produced greater cardiac toxicity. However, both IFO MDOs had a greater diversity of 4- and 5-ring PACs, with the IFO2 MDO having concentrations of fluoranthene and total 5-ring PACs (e.g. benzo[*a*]pyrene) that were 2 times as high as those in the ANSCO MDO. These PACs are capable of contributing to developmental abnormalities of the heart through mechanisms that are different than those that mediate the cardiotoxicity of tricyclic compounds (see Section 4).

One novel type of sublethal toxicity consistently observed with dark exposures to IFO1 was an effect on tail development. Exposure to ANSCO typically causes a delay or reduced outgrowth of the finfolds (Fig. 1B and Incardona et al., 2005), which later manifests as finfold blisters (Incardona et al., 2005). In addition to reduced outgrowth of the entire caudal finfold, embryos exposed to IFO1 displayed at 72 hpf a high frequency (>50%) of a different defect characterized by a notch on its dorsal side (Fig. 2D). This type of defect was not observed with IFO2.

3.3. Sunlight initiates acute cell-lethal toxicity following exposure to IFOs but not ANSCO

The potential for photoinduced toxicity from sunlight (i.e., UV) exposure was tested in 5 experiments under very different weather regimes from July to December 2008 (Table 1). In each experiment there was a dramatic and acute lethal toxicity induced by subsequent sunlight exposure observed with the 2 residual IFOs (Figs. 2, 3 and S2 and Table 4), but not the unrefined ANSCO. Embryonic exposure to either IFO1 (Fig. 2) or IFO2 (Fig. S2), followed by sunlight exposure at either 48 hpf or 72 hpf, resulted in a rapid and severe lytic deterioration of the caudal finfold, sometimes involving the entire tail (Fig. 2E, 72 hpf). Finfold cytolysis was discernable within minutes of terminating the sunlight exposure, and in some cases

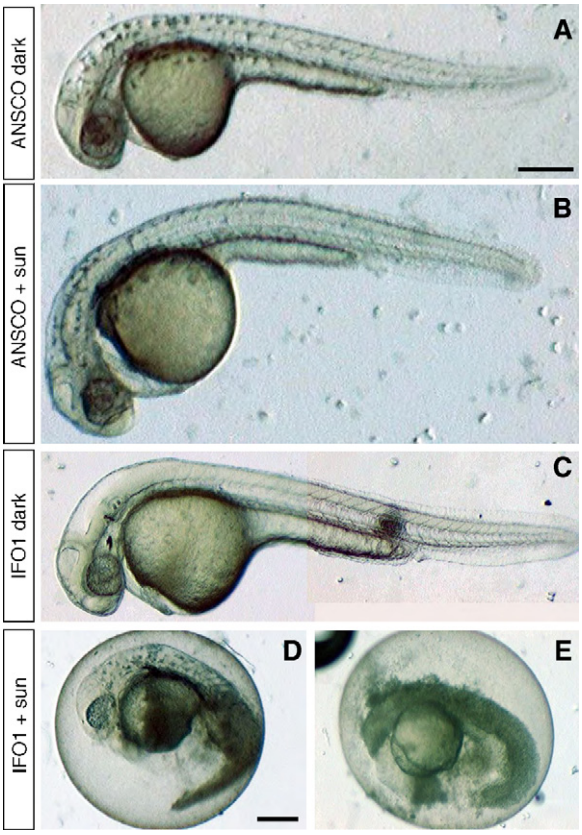

Fig. 3. Phototoxicity is enhanced by lack of pigment cells. Embryos were exposed to MDO preparations from 6 to 24 hpf, exposed to sunlight or outdoor ambient temperature in the dark for 120 min, then returned indoors and imaged (experiment 3, 7 October). Dechorionated embryos are shown in A–C with the head to the left; embryos in D and E were left in the chorion due to their deteriorating condition. (A) Embryo exposed to ANSCO without sunlight. (B) Embryo exposed to ANSCO followed by sunlight. (C) Embryo exposed to IFO1 without sunlight (D) and (E) embryos exposed to IFO1 followed by sunlight exposure. Note the necrosis of the entire posterior half of the embryo in (D) and the entire embryo in (E). Scale bars are 0.5 mm.

had evidently commenced prior to the end of sunlight exposure. This effect was observed in all 5 experiments, and differed only in degree of severity, but was absent in ANSCO-exposed embryos (Fig. 2C).

By 48 hpf normal zebrafish embryos develop large numbers of black pigment-containing melanophores in the head and trunk, but not the finfolds. To determine if light-absorbing natural skin pigments provided protection from photoinduced oil toxicity, we tested either 24 hpf embryos (prior to melanophore development) or 48 hpf *nacre* larvae (a mutant with markedly reduced melanophores). Despite shorter exposure to MDOs, cytolytic effects were much more severe in 24 hpf embryos exposed to IFO1 (Fig. 3D and E), and the lytic response to both IFO MDOs in *nacre* larvae at 48 hpf often involved tissues in the head and trunk (Fig. S2 and data not shown). While sunlight did not produce phototoxicity in 24 hpf embryos exposed to ANSCO (Fig. 3B), with IFO1 exposure, large portions of the trunk (Fig. 3D) and sometimes the entire embryo (Fig. 3E) would undergo cytolysis.

In the MDO preparations where quantification of phototoxicity was paired with analyses for PACs, the $\sum$ PAC levels and composition were comparable (Table 2). The ANSCO and IFO1 MDOs had $\sum$ PAC of 210 and 240 μg/l, respectively, while the IFO2 MDO had 440 μg/l largely due to a 2-fold higher level of naphthalenes. Nevertheless, the cytolytic response to sunlight exposure was absent in embryos exposed to ANSCO (Table 4). In this experiment, the most marked differences between MDO preparations of ANSCO and the

Table 4
Summary of toxicity results.[a].

Assay	Control	ANSCO (ΣPACs)	IFO1 (ΣPACs)	IFO2 (ΣPACs)
Defects with dark incubator exposure				
Edema (mean percent ± SEM; overall mean of 4 experiments)	8 ± 6	88 ± 2	68 ± 16	100
Edema (experiment 7, mean percent ± SEM, $n = 3$)	11 ± 1	80 ± 0 (210)	100 (240)	100 (440)
Edema (experiment 8, mean percent ± SEM, $n = 3$)	5 ± 0	90 ± 5 (340)	93 ± 8 (100)	100 (310)
Tail defect (experiment 7, single replicate)	0	5	45	0
Phototoxicity (experiment 7, single replicate)				
Rounding of inner finfold cells	0	0	50	50
Lysis of outer finfold	0	0	45	50
Lysis of inner tail cells	0	0	5	0

[a] To compare toxicity to water chemistry for edema response, ΣPACs are shown in parentheses for each oil in the experiments where edema response quantification was paired with PAC analysis.

residual fuel oils among the conventionally measured PACs were the higher concentrations of 4- and 5-ring compounds. In particular, the total concentrations of fluoranthenes and chrysenes were 3–4 times higher in the IFO MDOs (12 and 18 μg/l vs. 4 μg/l). However, the IFO1 MDO produced slightly more severe tail damage, despite having lower concentrations of 4- and 5-ring compounds than the IFO2 MDO.

4. Discussion

As would be expected from the overall PAH compositions, the canonical cardiogenic edema response was observed after exposure to each of the three oil types in the absence of light. However, there were important differences between the magnitude of the response in relation to the PAC concentrations and composition of the corresponding MDO preparations, especially the concentrations of tricyclic PACs. For example, although IFO1 and ANSCO both produced edema in ~90% of embryos in 1 experiment, the concentrations of $\sum$ PACs and tricyclic PACs in IFO1 were ~17–44% of those in ANSCO and IFO2. This suggests that compounds other than the tricyclic PACs contributed to the edema response from IFO1. The higher molecular weight PACs that are generally more abundant in the IFOs are a likely candidate, including benz[*a*]anthracence, fluoranthene, and benzo[*a*]pyrene, as they also are capable of causing pericardial edema through a different mechanism (Incardona et al., 2006; Matson et al., 2008; Wills et al., 2009; our unpublished observations). Similarly, the relatively abundant carbazoles in the IFOs are likely act synergistically to increase the embryotoxicity of other PACs (Wassenberg et al., 2005). The pericardial edema resulting from IFO exposure most likely has a more complicated etiology than the response from ANSCO exposure, consistent with the greater complexity of compounds. The etiology of the novel tail defect associated with exposure to IFO1 is unclear, because most of the compounds identified as enriched in IFO1 relative to ANSCO were common to both IFOs. However, our chemical analysis was not comprehensive, and we did not characterize polar and other potentially toxic compounds that may also be present in the residual fuel oils. Because the overall toxicity and chemistry of the 2 IFO 380s tested here were grossly similar, it is likely that inclusion of a larger number residual fuel oils would reveal even greater toxicological heterogeneity.

In general, only sublethal effects (e.g. pericardial edema, fin malformation) are observed as an acute response in fish embryos exposed to oiled water preparations (as an individual stressor) that have $\sum$ PAC concentrations in the ranges reported here. In contrast, the addition of sunlight as a co-stressor converted the toxicity of the 2 IFOs but not ANSCO to produce rapid and overt lethality through a cytotoxic mechanism. The rapid cell death observed in the finfold and tail tissue within minutes to an hour after sunlight exposure is most consistent with a photoinduced cytolytic response due to plasma membrane damage, rather than an apoptotic mechanism. This is particularly supported by our finding that this enhanced oil toxicity is ameliorated by the presence of light-absorbing, melanin-containing pigment cells in the skin of zebrafish embryos. However, the precise mechanisms leading to membrane damage cannot be determined from these data. Several studies in both cell lines and in intact animals have shown that photoactivation of PACs leads to general membrane damage through lipid peroxidation (Kagan et al., 1987; McCloskey and Oris, 1993; Weinstein et al., 1997). While membrane lipid peroxidation is a well-known action of other non-PAC phototoxic compounds (Girotti and Deziel, 1983), some compounds associated with photoinduced cytolysis may act through oxidation of membrane proteins (Cardenas et al., 1992).

In a previous study, ANSCO was found to produce lethal phototoxicity when combined with sunlight or artificial UV exposure in herring larvae, but not embryos (Barron et al., 2003). Our study was not designed to replicate these results, and there are key differences. First, our results with zebrafish embryos and ANSCO are consistent with the results with herring embryos, and may relate to the toxicokinetic differences between early embryos and larvae. Second, the UV-A doses from sunlight in the previous study ranged from 2160 to 3600 μW h/cm^2, while in this study the range was 290–1790 μW h/cm^2. Finally, lethality was quantified over a number of days in the former study, while here acute lethality was assessed only immediately after sunlight exposure. The marked differences between the two IFO 380s and ANSCO in phototoxic potential observed here is most likely due to distinct chemical differences between residual fuel oils and crude oil.

While our preliminary analysis of the IFO 380 MDO preparations identified a large number of additional compounds, these particular compounds may or may not be responsible for the markedly different phototoxicity. Although the elevated phototoxicity of the IFOs could be due to the higher concentrations of fluoranthenes and chrysenes alone, this seems unlikely. The differences in total fluoranthenes and chrysenes (and 5-ring compounds) between the various MDOs were not large (e.g. only 3 times greater in IFO1 vs. ANSCO). If these compounds alone were responsible for the dramatic phototoxicity of the IFOs, then there must be a very sharp threshold that is not far above the concentrations present in the ANSCO MDOs. The other heterocyclic PACs identified in the IFOs (e.g. the benzothiophenes and carbazoles) are unlikely to be phototoxic alone (Kochevar et al., 1982). A more parsimonious explanation is that these PACs contribute to the phototoxicity in combination with some of the other identified or unidentified compounds that are present at higher concentrations in the IFOs. Despite the wide range of compounds included in our analysis, it is likely that an even more comprehensive analysis is necessary to identify the compounds responsible for the potent phototoxicity of these IFOs.

These results indicate that, compared to crude oil, residual fuel oils can produce different sublethal toxicity (e.g. tail defects), and that at least 2 individual IFOs have the potential to produce dramat-

ically lethal toxicity among translucent animals in the presence of sunlight. Moreover, the canonical response of cardiogenic edema is likely to arise through more than one mechanism, depending on the relative ratios of PACs that act through different (e.g. aryl hydrocarbon receptor-independent and -dependent) mechanisms. Our findings identify a number of compounds beyond the conventionally studied PACs that should be targeted for further toxicity studies, in particular the heterocyclic compounds which are enriched in residual fuel oils. Finally, this study highlights the need for a broader approach to understanding the toxicity of diverse oil types to better assess the ecological impacts of oil spills, especially in areas where additional stressors such as intense solar radiation may exist.

Acknowledgements

The authors thank Susan Sugarman (OSPR) for providing the IFO1 sample and Sven Christensen (Olympic Tug and Barge) for providing the IFO2 sample, Mark Carls for providing the radiometer, Tiffany Linbo for zebrafish husbandry, Gina Ylitalo, Jim Meador, and Jana Labenia for critical reviews of the manuscript. This work was supported by NOAA Fisheries programatic funds and the authors are solely responsible for the experimental design, implementation, data analysis and interpretation.

Appendix A. Supplementary data

Supplementary data associated with this article can be found, in the online version, at doi:10.1016/j.aquatox.2010.04.002.

References

Arfsten, D.P., Schaeffer, D.J., Mulveny, D.C., 1996. The effects of near ultraviolet radiation on the toxic effects of polycyclic aromatic hydrocarbons in animals and plants: a review. Ecotoxicol. Environ. Saf. 33, 1–24.

Barron, M.G., Carls, M.G., Short, J.W., Rice, S.D., 2003. Photoenhanced toxicity of aqueous phase and chemically dispersed weathered Alaska North Slope crude oil to Pacific herring eggs and larvae. Environ. Toxicol. Chem. 22, 650–660.

Barron, M.G., Ka'aihue, L., 2001. Potential for photoenhanced toxicity of spilled oil in Prince William Sound and Gulf of Alaska Waters. Mar. Pollut. Bull. 43, 86–92.

Barron, M.G., Podrabsky, T., Ogle, S., Ricker, R.W., 1999. Are aromatic hydrocarbons the primary determinant of petroleum toxicity to aquatic organisms? Aquat. Toxicol. 46, 253–268.

Cardenas, A.M., Cortes, M.P., Fernandez, E., Pena, W., 1992. Lipid peroxidation and loss of potassium from red blood cells produced by phototoxic quinolones. Toxicology 72, 145–151.

Carls, M.G., Holland, L., Larsen, M., Collier, T.K., Scholz, N.L., Incardona, J.P., 2008. Fish embryos are damaged by dissolved PAHs, not oil particles. Aquat. Toxicol. 88, 121–127.

Carls, M.G., Meador, J.P., 2009. A Perspective on the toxicity of petrogenic PAHs to developing fish embryos related to environmental chemistry. Hum. Ecol. Risk Assess. 15, 1084–1098.

Clark, R.C.J., Brown, D.W., 1977. Petroleum: properties and analyses in biotic and abiotic systems. In: Malins, D.C. (Ed.), Effects of Petroleum on Arctic and Subarctic Marine Environments and Organisms, vol. I. Academic Press, Inc, New York, pp. 1–89.

Cleveland, L., Little, E.E., Calfee, R.D., Barron, M.G., 2000. Photoenhanced toxicity of weathered oil to *Mysidopsis bahia*. Aquat. Toxicol. 49, 63–76.

Diamond, S.A., Mount, D.R., Mattson, V.R., Heinis, L.J., Highland, T.L., Adams, A.D., Simcik, M.F., 2006. Photoactivated polycyclic aromatic hydrocarbon toxicity in medaka (*Oryzias latipes*) embryos: relevance to environmental risk in contaminated sites. Environ. Toxicol. Chem. 25, 3015–3023.

Duesterloh, S., Short, J.W., Barron, M.G., 2002. Photoenhanced toxicity of weathered Alaska north slope crude oil to the calanoid copepods *Calanus marshallae* and *Metridia okhotensis*. Environ. Sci. Technol. 36, 3953–3959.

Farwell, A.J., Nero, V., Croft, M., Rhodes, S., Dixon, D.G., 2006. Phototoxicity of oil sands-derived polycyclic aromatic compounds to Japanese medaka (*Oryzias latipes*) embryos. Environ. Toxicol. Chem. 25, 3266–3274.

Girotti, A.W., Deziel, M.R., 1983. Photodynamic action of protoporphyrin on resealed erythrocyte membranes: mechanisms of release of trapped markers. Adv. Exp. Med. Biol. 160, 213–225.

González-Doncel, M., Gonzalez, L., Fernández-Torija, C., Navas, J.M., Tarazona, J.V., 2008. Toxic effects of an oil spill on fish early life stages may not be exclusively associated to PAHs: studies with Prestige oil and medaka (*Oryzias latipes*). Aquat. Toxicol. 87, pp. 280–268.

Incardona, J.P., Carls, M.G., Day, H.L., Sloan, C.A., Bolton, J.L., Collier, T.K., Scholz, N.L., 2009. Cardiac arrhythmia is the primary response of embryonic Pacific herring (*Clupea pallasi*) exposed to crude oil during weathering. Environ. Sci. Technol. 43, 201–207.

Incardona, J.P., Carls, M.G., Teraoka, H., Sloan, C.A., Collier, T.K., Scholz, N.L., 2005. Aryl hydrocarbon receptor-independent toxicity of weathered crude oil during fish development. Environ. Health Perspect. 113, 1755–1762.

Incardona, J.P., Collier, T.K., Scholz, N.L., 2004. Defects in cardiac function precede morphological abnormalities in fish embryos exposed to polycyclic aromatic hydrocarbons. Toxicol. Appl. Pharmacol. 196, 191–205.

Incardona, J.P., Day, H.L., Collier, T.K., Scholz, N.L., 2006. Developmental toxicity of 4-ring polycyclic aromatic hydrocarbons in zebrafish is differentially dependent on AH receptor isoforms and hepatic cytochrome P450 1A metabolism. Toxicol. Appl. Pharmacol. 217, 308–321.

Kagan, J., Stokes, A., Gong, H.H., Tuveson, R.W., 1987. Light-dependent cytotoxicity of fluoranthene: oxygen-dependent membrane damage. Chemosphere 16, 2417–2422.

Kochevar, I.E., Armstrong, R.B., Einbinder, J., Walther, R.R., Harber, L.C., 1982. Coal tar phototoxicity: active compounds and action spectra. Photochem. Photobiol. 36, 65–69.

Kováts, E., 1958. Gas-chromatographische charakterisierung organischer verbindungen. Teil 1: retentions indices aliphatischer halogenide, alkohole, aldehyde und ketone. Helv. Chim. Acta 41, 1915–1932.

Kováts, E., 1965. Gas chromatographic characterization of organic substances in the retention index system. Adv. Chromatogr. 1, 229–247.

Linbo, T.L., 2009. Zebrafish (*Danio rerio*) husbandry and colony maintenance at the Northwest Fisheries Science Center. NOAA Technical Memorandum. U.S. Department of Commerce, p. 75.

Lister, J.A., Robertson, C.P., Lepage, T., Johnson, S.L., Raible, D.W., 1999. nacre encodes a zebrafish microphthalmia-related protein that regulates neural-crest-derived pigment cell fate. Development 126, 3757–3767.

Matar, S., Hatch, L.F., 2001. Chemistry of Petrochemical Processes. Gulf Professional Publishing, Boston, p. 356.

Matson, C.W., Timme-Laragy, A.R., Di Giulio, R.T., 2008. Fluoranthene, but not benzo[a]pyrene, interacts with hypoxia resulting in pericardial effusion and lordosis in developing zebrafish. Chemosphere 74, 149–154.

McCloskey, J.T., Oris, J.T., 1993. Effect of anthracene and solar ultraviolet radiation exposure on gill ATPase and selected hematologic measurements m the bluegill sunfish (*Lepomis macrochirus*). Aquat. Toxicol. 24, 207–218.

Neff, J.M., Ostazeski, S., Gardiner, W., Stejskal, I., 2000. Effects of weathering on the toxicity of three offshore Australian crude oils and a diesel fuel to marine animals. Environ. Toxicol. Chem. 19, 1809–1821.

Oris, J.T., Giesy, J.P., 1987. The photo-induced toxicity of polycyclic aromatic hydrocarbons to larvae of the fathead minnow (*Pimephales promela*). Chemosphere 16, 1395–1404.

Payne, J.R., Reilly, T.J., French, D.P., 1999. Fabrication of a portable large-volume water sampling system to support oil spill NRDA efforts. In: Proceedings of the 1999 International Oil Spill Conference. American Petroleum Institute, Washington, DC, pp. 1179–1184.

Pelletier, M.C., Burgess, R.M., Ho, K.T., Kuhn, A., McKinney, R.A., Ryba, S.A., 1997. Phototoxicity of individual polycyclic aromatic hydrocarbons and petroleum to marine invertebrate larvae and juveniles. Environ. Toxicol. Chem. 16, 2190–2199.

Peterson, C.H., Rice, S.D., Short, J.W., Esler, D., Bodkin, J.L., Ballachey, B.E., Irons, D.B., 2003. Long-term ecosystem response to the Exxon Valdez oil spill. Science 302, 2082–2086.

Sloan, C.A., Brown, D.W., Pearce, R.W., Boyer, R.H., Bolton, J.L., Burrows, D.G., Herman, D.P., Krahn, M.M., 2005. Determining aromatic hydrocarbons and chlorinated hydrocarbons in sediments and tissues using accelerated solvent extraction and gas chromatography/mass spectrometry. In: Ostrander, G.K. (Ed.), Techniques in Aquatic Toxicology, vol. 2. CRC Press, Boca Raton, FL, pp. 631–651.

Uhler, A.D., Stout, S.A., Douglas, G.S., 2007. Chemical heterogeneity in modern marine residual fuel oils. In: Wang, Z., Stout, S.A. (Eds.), Oil Spill Environmental Forensics. Academic Press, London, pp. 327–348.

Wang, Z., Hollebone, B.P., Fingas, M., Fieldhouse, B., Sigouin, L., Landriault, M., Smith, P., Noonan, J., Thouin, G., Weaver, J.W., 2003. Characteristics of Spilled Oils, Fuels, and Petroleum Products: 1. Composition and Properties of Selected Oils. U.S. Environmental Protection Agency, Washington, D.C.

Wassenberg, D.M., Nerlinger, A.L., Battle, L.P., Di Giulio, R.T., 2005. Effects of the polycyclic aromatic hydrocarbon heterocycles, carbazole and dibenzothiophene, on in vivo and in vitro CYP1A activity and polycyclic aromatic hydrocarbon-derived embryonic deformities. Environ. Toxicol. Chem. 24, 2526–2532.

Weinstein, J.E., Oris, J.T., Taylor, D.H., 1997. An ultrastructural examination of the mode of UV-induced toxic action of fluoranthene in the fathead minnow, *Pimephales promelas*. Aquat. Toxicol. 39, 1–22.

Wills, L.P., Zhu, S., Willett, K.L., Di Giulio, R.T., 2009. Effect of CYP1A inhibition on the biotransformation of benzo[a]pyrene in two populations of *Fundulus heteroclitus* with different exposure histories. Aquat. Toxicol. 92, 195–201.

Yu, H., 2002. Environmental carcinogenic polycyclic aromatic hydrocarbons: photochemistry and phototoxicity. J. Environ. Sci. Health C: Environ. Carcinog. Ecotoxicol. Rev. 20, 149–183.